Thermal Diffusivity Measurement of SnO$_2$-CuO Ceramic at Room Temperature

Aiza M.M.*, Zaidan A.W., Wan Mahmood M.Y. and Norfarezah H.E.
Applied Optics Laboratory, Department of Physics, Faculty of Science,
Universiti Putra Malaysia, 43400 UPM, Serdang, Selangor, Malaysia
*E-mail: masya197@yahoo.com.sg

ABSTRACT

Thermal diffusivity is a measure of rapidity of heat propagation through a material. The property is important in the understanding of gas sensor performance. Photoflash technique was used to determine thermal diffusivity of SnO$_2$-based materials with varying amount of CuO ranging from 10 to 50 mol%, at room temperature. The samples were made disc-shaped, 10 mm in diameter with thickness ranging from 2.4 to 2.8 mm. We found that the thermal diffusivity values of SnO$_2$-CuO samples ranging from 6.21 to 7.51×10^{-2} cm^{2}s^{-1} were better than the reported thermal diffusivity value of pure SnO$_2$ sample (1.45×10^{-2} cm^{2}s^{-1}). The thermal diffusivity behaviour was supported by results from XRD and SEM.

Keywords: Photoflash technique, SnO$_2$-CuO, thermal diffusivity

INTRODUCTION

Atmospheric pollution and safety requirements for industry have led to research and development of a variety of gas sensors using different materials and technologies particularly for better sensor performance (Chang *et al.*, 2002). An n-type semiconducting oxide such as tin dioxide (SnO$_2$) is one of the most important and extensively used materials for the detection of a number of toxic gases (Saadeddin *et. al.*, 2006, Vasiliev *et al.*, 1998). It is well established that the SnO$_2$-based gas sensors offer desirable attributes of cheapness, simplicity and high sensitivity (Kocemba *et al.*, 2001). However, there are some limitations to the wide use of semiconductor gas sensors i.e. lack of selectivity, long term drift and sensitivity to air humidity. The improvement of sensor properties of these materials can be achieved by the addition of adequate dopants.

Thermal diffusivity, α, is a measure of rapidity of the heat propagation through a material. The higher the value of thermal diffusivity of a material, the faster will be the heat propagation. For gas sensor application, it is important to first heat up the sensor to its operating temperature in order to activate the gas sensing property. For the sensor to be immediately used, we need the sensor to reach its operating temperature in a short time. So, sensors with higher thermal diffusivity material will give faster initialization time than sensors with lower thermal diffusivity. In this study, copper oxide, CuO was added to SnO$_2$ as the dopant to see its effects on the thermal diffusivity.

Nowadays, several different techniques for the determination of the thermal diffusivity may be found in the literatures. The proper method is usually selected by considering the

specimen size, shape, temperature characteristics and temperature range. The photoflash technique which has been developed by Parker *et al.* (1961) has been widely used due to the ease of sample preparation, less material requirements and fast measurements. One typically obtains accuracy within ± 5% when implementing careful measurement techniques.

MATERIALS AND METHODS

SnO_2-CuO ceramic was prepared using solid state route (Moon *et al.,* 2001). The raw materials used were SnO_2 (99.9%, Alfa Aesar) and CuO (extra pure, Scharlau). The details of the samples composition are shown in Table 1.

TABLE 1
Samples composition

Sample Name	Composition (mol%)	
	SnO_2	CuO
SC1	90	10
SC2	80	20
SC3	70	30
SC4	60	40
SC5	50	50

All the powders were weighed according to their compositions, wet mixed and stirred for 24 hours. The slurry was dried in an oven at 120°C for 10 hours. The mixtures were pre-sintered at 850°C for 2 hours at the heating and cooling rate of 3°Cmin⁻¹. The samples were sieved using 75 μm sieve. The green bodies were pressed into pellets of 10 mm in diameter with thickness ranging from 2.4 to 2.8 mm, at the pressure of 20 kN. Samples were then sintered at 1000°C for 3 hours.

The X-ray diffraction analysis was carried out for all samples using a Philip model 7602 EA Almelo X-ray Diffractometer (CuKα, λ=1.5418 Å) at range of 20 to 80 degree. The data was collected and analyzed with a Philips X'Pert Data Collector (Version 1.2d) software. The microstructure of the samples was observed by using a JEOL model 6400 Scanning Electron Microscope (SEM). To protect samples from charging by the electron beam during observation, the samples were coated with a thin gold film. Each sample was scanned at 10 kV accelerating voltage.

An important property of any material is its density. Measuring sample's density is one way to investigate the porosity of the sample. The increase of density for the sample could be due to the sufficient space or vacancies for an effective transportation of metal ions and the decrease of density could indicate the increased number and size of pores trapped within the grains. All sintered samples had their dimensions measured and were dry weighed. The geometrical density calculation is defined as:

$$D = \frac{m}{\pi\left(\dfrac{d}{2}\right)^2 L} \tag{1}$$

where *m, d* and *L* are the mass, diameter and thickness of the pellet sample, respectively. The theoretical density of the samples was calculated using the equation;

$$\rho_{theo} = \frac{m_s}{(V_{SnO_2} + V_{CuO})} \tag{2}$$

where ρ_{theo}, m_s, V_{SnO2} and V_{CuO} are the theoretical density, the mass of the mixture of sample, the volume fraction of SnO$_2$ and the volume fraction of CuO, respectively.

Thermal diffusivity of SnO$_2$-CuO ceramics was measured by using the photoflash technique at room temperature. The sample was polished using abrasive silicone carbide sandpaper to obtain a flat surface and also to get rid of impurities. Calibration was performed using standard Aluminium sample before starting the experiment. The schematic diagram of this technique is shown in *Fig. 1*. The front surface of the sample was exposed to a short burst of radiant energy from photoflash. The transient temperature curve of the rear surface of the sample was then measured with a thermocouple.

For photoflash technique, two ways of determining thermal diffusivity have been deduced by Parker *et al.* (1961) from the equation below.
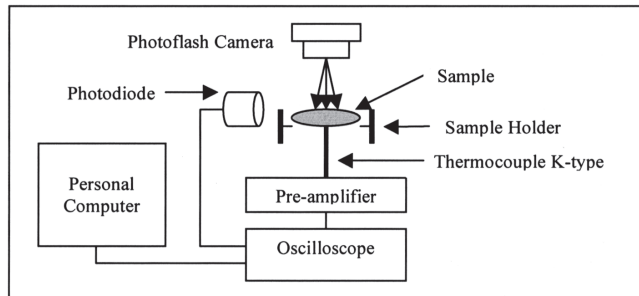

Fig. 1: Schematic diagram of the photoflash technique

$$V = 1 + 2\sum_{n=1}^{\infty} (-1)^n \exp(-n^2 w) \tag{3}$$

When V is equal to 0.5, ω is equal to 1.37, so

$$\alpha = 1.37 \frac{L^2}{\pi^2 t_{1/2}} \tag{4}$$

where t$_{1/2}$ is the time required for the back surface to reach half of the maximum temperature rise. Alternatively, t$_x$, the tangent to the temperature-time curve at the point of maximum gradient can be extrapolated to the time axis where the intercept, occur at ω = 0.48 from which

$$\alpha = 0.48 \frac{L^2}{\pi^2 t_x} \tag{5}$$

where t_x is the time axis intercept versus time curve. Actually we may also use any percentage rise as the reference point for the calculation of thermal diffusivity as given below:

$$\alpha = k_x \frac{L^2}{t_x} \tag{6}$$

where K_x is a constant corresponding to an x percentage rise of temperature at the rear surface of slab and t_x is the elapsed time to an x percentage rise.

In the calculation of thermal diffusivity, it is advisable to rely on a single point from the whole curve, as in the case with expression [4]. Expression [6] permits the use of the portion of the response curve, which has been least affected by interferences. The use of expression [6] is therefore strongly recommended.

The characteristics rise time is important in order to quantify whether the corrections for finite pulse effect should be applied to the measurement. For the finite pulse time effect considerations, the pulse duration, τ (5ms) of the photoflash was compared with the characteristic rise time, t_c of the sample. The finite pulse effect in this study was always less than 1 ($\tau/t_c \ll 1$), so the finite pulse time correction is negligible (Maglic *et al.* 1992).

Heat loss usually occurs in the flash method. Radiation heat loss corrections can be done based on Clark and Taylor (1975) rise-curve data by employing the ratio technique. For the $t_{0.75} / t_{0.25}$ ratio i.e, the time to reach 75% of the maximum divided by the time to reach 25% of the maximum, the ideal value of the ratio is 2.272. This ratio must be determined from the experimental data. Then the correction factor, K_R can be calculated from the equation

$$K_R = -0.3461467 + 0.361578\left(\frac{t_{0.75}}{t_{0.25}}\right) - 0.06520543\left(\frac{t_{0.75}}{t_{0.25}}\right)^2 \tag{7}$$

The corrected value of thermal diffusivity at the half time will be

$$\alpha_{corrected} \frac{\alpha_{0.5} K_R}{0.13885} \tag{8}$$

Besides that, corrections by using many other ratios can also be used if the constants for calculating the correction factor are provided.

RESULTS AND DISCUSSION

The phase composition analyzed by XRD, showed that there were no impurity phases in SnO_2-CuO system, *Fig. 2.* All peaks are presented by SnO_2 and CuO (Zhang and Liu, 2000). The absence of CuO peaks in the SC1 sample may be due to the smaller X-ray scattering power of CuO than SnO_2. The CuO peak was observed for SC_2, but the intensity of CuO peak remains low, suggesting that the concentration of CuO phase in SnO_2–CuO is small. Strong peaks of CuO (-111, 111) were observed in SC3 (at 2θ = 35.57°, 38.77°, respectively).The intensity of peaks corresponding to the CuO phases

increased slightly from SC3 to SC5 while SnO_2 peaks (110, 101, 211) at 2θ = 26.60°, 33.89° and 51.80°, respectively were gradually decreased when the concentration of CuO phase in SnO_2–CuO were increased.

Fig. 3 shows one of the thermograms obtained from the thermal diffusivity measurements. The rest of the data obtained in this study are presented in Table 2 which show the characteristic rise time and corrected thermal diffusivity, α_c value at different composition of CuO mixed with SnO_2. *Fig. 4* shows the relationship between thermal diffusivity and SnO_2–CuO system.
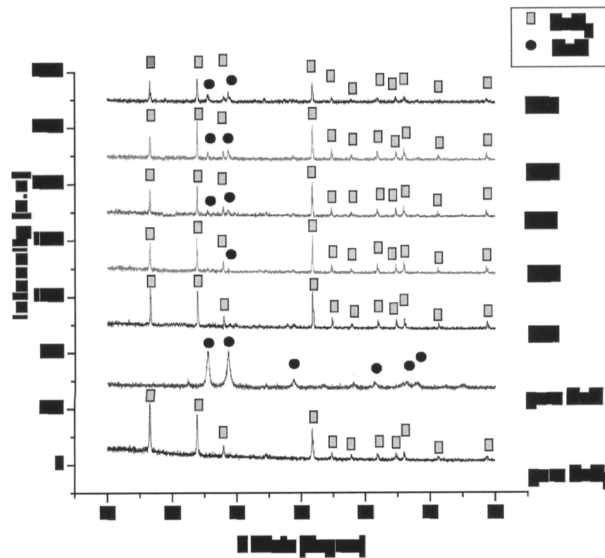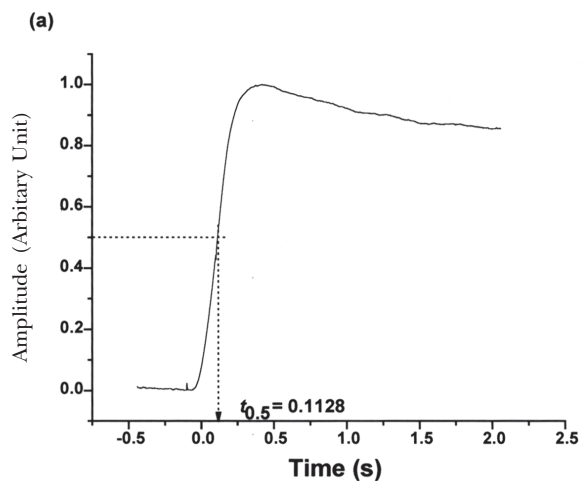

Fig. 2: XRD patterns of SnO2-CuO samples

Fig. 3: Thermogram of SC1 sample (thickness, L=0.2354 cm)
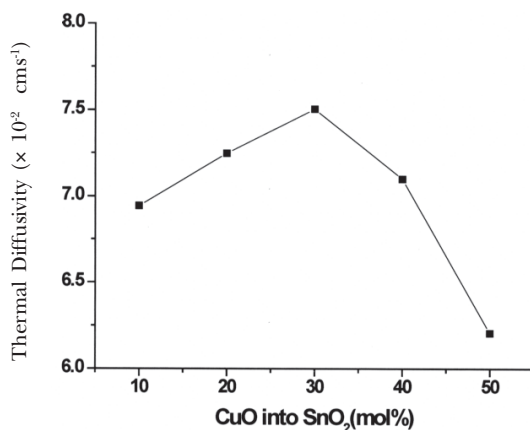
Pertanika J. Sci. & Technol. Vol. 16 (2) 2008

269

Fig. 4: Thermal diffusivity of SnO_2-CuO at different composition

TABLE 2
Characteristic rise time and the corrected thermal diffusivity value
of SnO_2-CuO at different composition

Sample	Thickness (cm)	Half rise time $t_{0.5}$ (s)	Characteristic rise time, $t_c = L^2/\alpha\pi^2$ (s)	τ / t_c (s)	Corrected thermal diffusivity, α_c ($\times 10^{-2}$ cm²s⁻¹)
SC1	0.2354	0.1128	0.0818	0.0611	6.9436
SC2	0.2325	0.1100	0.0803	0.0623	7.2468
SC3	0.2719	0.1484	0.1083	0.0462	7.5048
SC4	0.2722	0.1554	0.1132	0.0442	7.0995
SC5	0.2782	0.1758	0.1283	0.0390	6.2059

Thermal diffusivity of pure SnO_2 has been reported to be 1.45×10^{-2} cm²s⁻¹ (Rosyaini, 2004). The introduction of CuO (10-50 mol %) into the ceramic system, resulted in thermal diffusivity range of 6.21 to 7.51×10^{-2} cm² s⁻¹. The addition of CuO up to 30 mol% increased the thermal diffusivity value from 1.45×10^{-2} cm²s⁻¹ (pure SnO_2) to 7.51×10^{-2} cm² s⁻¹ (SC3). However, further addition of CuO beyond 30 mol% decreases thermal diffusivity value to 6.21×10^{-2} cm² s⁻¹.

The influence of CuO on the sintered samples densities, theoretical densities, relative densities and porosities is shown in Table 3 while *Fig. 5* shows the relative density as a function of mole percentage of CuO addition. *Fig. 6* shows the porosity percentage as a function of mole percentage of CuO addition.

Based on the density measurement, the density of the sintered sample decreases gradually as CuO was increased (10-50 mol%). The highest density (ρ = 5.87 gcm⁻³), was obtained for the SC1 sample where its relative density was about 85% of the theoretical density, while SC5 gave the lowest density (ρ = 5.39 gcm-3) where its relative density was about 80% of the theoretical density. This indicates that more pores were present in this sample as more CuO was introduced.

It is well understood that heat propagation will be retarded as they encounter grain boundaries. Every grain boundary is a potential site for phonon scattering. For heat

TABLE 3
Influence of CuO on the sintered samples densities, theoretical densities,
relative densities and porosities

Sample	Sintered Density (gcm^{-3})	Theoretical Density (gcm^{-3})	Relative Density (%)	Porosity (%)
SC1	5.87	6.92	84.86	15.14
SC2	5.72	6.89	83.04	16.96
SC3	5.63	6.85	82.09	17.91
SC4	5.46	6.81	80.07	19.93
SC5	5.39	6.77	79.63	20.37
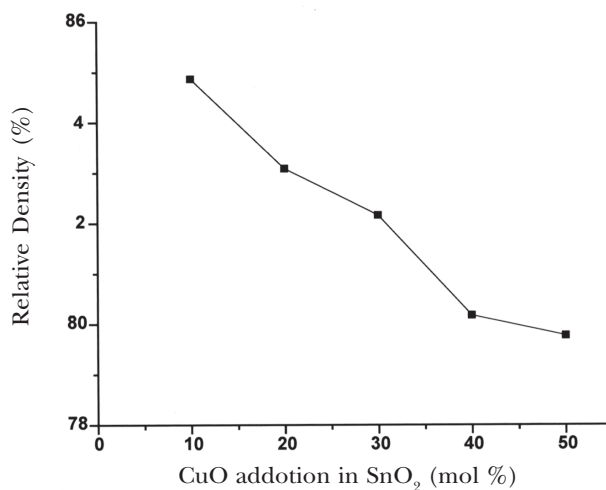
Fig. 5: Influence of CuO addition to relative density
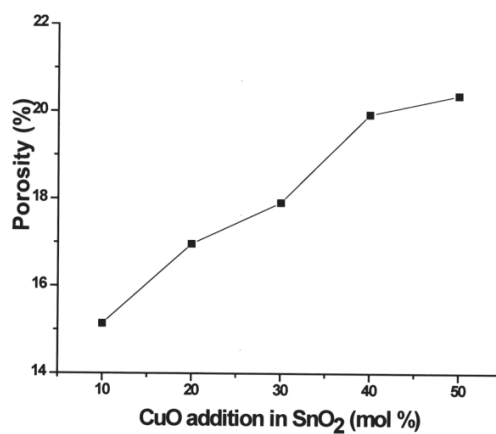
Fig. 6: Influence of CuO addition to porosity

Pertanika J. Sci. & Technol. Vol. 16 (2) 2008

271

propagation in two samples with two different grain sizes at a same micrometer distance, the one with bigger grain size will have less grain boundaries for the heat propagation to encounter than the other sample with smaller grain size which has more grain boundaries to be encountered. Hence, phonon scattering will be less in the sample with bigger grain size; thus will show higher thermal diffusivity value. This is in agreement with the SEM micrographs in *Fig. 7*. *Fig. 7(a), (b)* and *(c)* represent 10 mol%, 20 mol% and 30 mol% CuO mixed with SnO_2 respectively. It shows that the particle size of these compositions was getting slightly bigger as we increased CuO from 10-30 mol% in SnO_2 samples. Therefore the addition of CuO (10-30 mol%) had contributed to the increase in the thermal diffusivity values. However, the thermal diffusivity values keep decreasing as more CuO (40-50 mol%) were doped into SnO_2 samples. The decrease in density and an increase in porosity as evidenced in SEM micrograph in *Fig. 7(d)* and *(e)*, resulted in the decrease in thermal diffusivity of the sample with more than 40 mol% CuO.
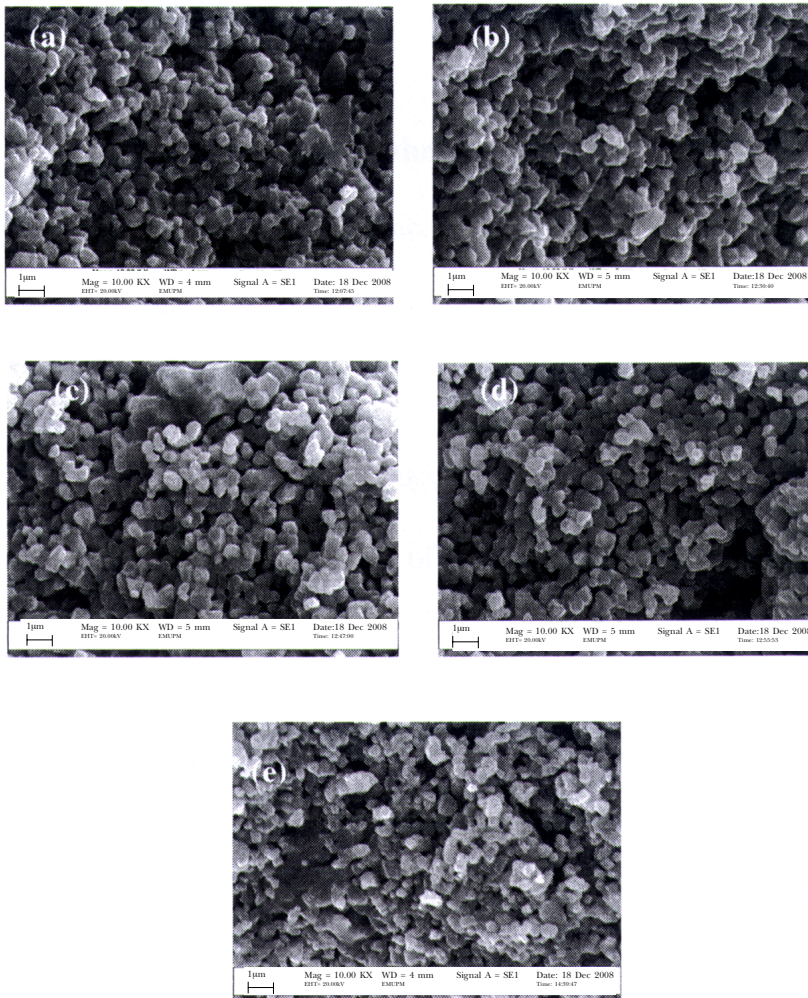

Fig. 7: SEM micrograph of fractured SnO2-CuO samples at different composition (a)10 mol% CuO (b) 20 mol% CuO (c) 30 mol% CuO (d) 40 mol% CuO (e) 50 mol% CuO, at 10,000 magnification

CONCLUSIONS

The influence of CuO used as additive (10-50 mol%) on the thermal and micro-structural properties of the SnO$_2$-based ceramics were studied. The phase composition analyzed by XRD, showed that there was no impurity phases in SnO$_2$-CuO system. We found that thermal diffusivity values of SnO$_2$-CuO samples ranging from 6.21 to 7.51 × 10-2 cm^2 s^{-1} which is better from the reported thermal diffusivity value of pure SnO$_2$ i.e 1.45 × 10^{-2} cm^2 s^{-1}. So, better performance of SnO$_2$ gas sensor in terms of thermal diffusivity, can be achieved by introducing 30 mol% CuO into SnO$_2$. The thermal diffusivity behavior was explained based on the crystallite aspect and density-porosity effect and it was supported by SEM micrographs.

ACKNOWLEDGEMENTS

REFERENCES

CHANG, J.F. ET AL. (2002). The effects of thickness and operation temperature on ZnO:Al thin film CO gas sensor. *Sensors and Actuators B, 84,* 258-264.

CLARK, L.M. and TAYLOR, R.E. (1975). Radiation loss in the flash method for thermal diffusivity. *Journal of Applied Physics, 46,* 714-719.

KOCEMBA, I. ET AL. (2001). The properties of strongly pressed tin oxide-based gas sensors. *Sensors and Actuators B, 79,* 28-32.

MAGLIC, K.D. ET AL. (1992). *Compendium of Thermophysical Property Measurement Methods.* Plenum Press.

MOON, W.J. ET AL. (2001). Selective CO gas detection of SnO$_2$-Zn$_2$SnO$_4$, *Sensors and Actuators B, 80,* 21-27.

PARKER, W.J. ET AL. (1961). Flash method of determining thermal diffusivity, heat capacity and thermal conductivity. *J. Appl. Phys., 32.*

ROSYAINI, A.Z. (2004). Sensor characteristic studies and thermal diffusivity measurement of tin (IV) oxide-based ceramic gas sensors (MSc. Thesis, Universiti Putra Malaysia, 2004).

SAADEDDIN ET AL. (2006). Simultaneous doping of Zn and Sb in SnO2 ceramics: enhancement of electrical conductivity. *Solid State Sciences, 8,* 7-13.

VASILIEV ET AL. (1998). CuO/SnO2 thin film heterostructures as chemical sensors to H2S. *Sensors and Actuators B, 50,* 186-193.

ZHANG, G., and LIU, M. (2000). Effect of particle size and dopants on properties of SnO2 based gas sensor. *Sensors and Actuators B, 69,* 144-152.